DYNAMICS OF MAGNETIC AND VELOCITY FIELDS IN CORONAL LOOPS

V.Krishan
Indian Institute of Astrophysics
Bangalore 560034, India

M.Berger and E.R.Priest
Mathematical Institute, University of St.Andrews
St.Andrews KY169SS, Fife, Scotland

ABSTRACT

The coronal loop plasma is represented by a superposition of the three lowest order Chandrasekhar-Kendall modes. The temporal evolution of the velocity and magnetic field in each of these mode is determined using ideal MHD equations under two simplified cases viz (i) allowing small departures from the equilibrium and (ii) the pump approximation.

1. INTRODUCTION

The structure of the velocity and magnetic fields plays a pivotal role in determining the heating, stability and evolution of the plasma in coronal loops (Athay and Klimchuk, 1987; Priest 1982, Krishan 1983 and 1985). In earlier studies, the pressure structure of the loop plasma was delineated using a Chandrasekhar-Kendall (C-K) representation of the velocity and magnetic field (Krishan 1983, 1985). This was done under the steady state assumption and therefore no information on the temporal behaviour of the fields and of the pressure could be derived. In this paper, we study the dynamics of the velocity and magnetic fields using ideal MHD equations and a Chandrasekhar-Kendall representation. The complete dynamics is described by a set of infinite, coupled nonlinear ordinary differential equations which are first order in time for the expansion coefficients of the velocity and magnetic field. Since obtaining the full solution of these equations is a formidable task, we choose to represent loop behaviour by a superposition of the three lowest order C-K functions. One justification for doing so is that these functions represent the largest spatial scales and therefore they may be the most suitable states for comparison with observed phenomena, if at all. This system reduces to a set of six equations, three for velocity and three for magnetic field. Solving these equations is again a formidable task without the help of a computer. However, analytical progress can be made in two simplified cases:
(i) when the system is disturbed linearly from its state of equilibrium and (ii) when one of the three modes has an amplitude much

larger than the other two. This is known as the Pump approximation. In the first case, one finds the disturbed fields undergoing sinusoidal oscillations with a period which is a function of the equilibrium amplitudes of the three modes. This may be one way of explaining the quasi-periodic oscillations observed in x-ray, microwave and EUV emissions from coronal loops.

In the second case, for special values of the initial amplitudes the system exhibits sinusoidal oscillations. However, under general intial conditions, the velocity and magnetic fields go through periods of growth, reversal, decay and saturation.

In the most general case, with arbitrary initial conditions, the set of six equations can be solved numerically. The velocity and magnetic field show a rather complex temporal structure, the interpretation of which would sometimes be done more appropriately using the language and concepts of chaotic phenomena. Although conservative systems display no attracting regions in phase space, no attracting fixed points, no attracting limit cycles and no strange attractors, nevertheless one also finds chaos: i.e. there are strange or chaotic regions in phase space, but they are not attractive and can be densely interweaved with regular regions. In general one is interested in the long-time behaviour of conservative systems in order to make use of the ergodic principle for a system with finite degrees of freedom. In addition, the motion in phase space is expected to be extremely complicated and this may have important relationship with the variety of observed sporadic phenomena.

2. NONLINEARLY INTERACTING MHD SYSTEM

The coupling of the velocity field $\vec{V}$ and the magnetic field $\vec{B}$ (in units of V) in a perfectly conducting incompressible fluid can be described by the ideal MHD equations:

$$\frac{\partial \vec{V}}{\partial t} + (\vec{V}.\vec{\nabla})\vec{V} = -\vec{\nabla} p + (\vec{\nabla}\times\vec{B})\times\vec{B} \tag{1}$$

$$\frac{\partial \vec{B}}{\partial t} = \vec{\nabla}\times(\vec{V}\times\vec{B}) \tag{2}$$

$$\vec{\nabla}.\vec{V} = 0 \quad ; \quad \vec{\nabla}.\vec{B} = 0 \tag{3}$$

where p is the mechanical pressure in units of V^2. In cylindrical geometry, the boundary conditions on $\vec{B}$ and $\vec{V}$ for a rigid and perfectly conducting surface at r = R are:

$$\begin{aligned} V_r &= 0 \text{ at } r = R \\ B_r &= 0 \text{ at } r = R \end{aligned} \tag{4}$$

We represent $\vec{V}$ and $\vec{B}$ by Chandrasekhar-Kendall functions as:

$$\vec{V} = \sum_{n,m} \lambda_{nm} \eta_{nm}(t) \vec{A}_{nm}(\vec{r})$$
$$\vec{B} = \sum_{n,m} \lambda_{nm} \xi_{nm}(t) \vec{A}_{nm}(\vec{r}) \tag{5}$$

where,

$$\vec{A}_{nm}(\vec{r}) = C_{nm} \vec{a}_{nm}(\vec{r})$$

$$\int d^3r \;\; \vec{A}^*_{nm} \cdot \vec{A}_{n'm'}(\vec{r}) = \delta_{nn'} \delta_{mm'}$$

and

$$\vec{a}_{nm}(\vec{r}) = \hat{e}_r \left(\frac{im}{r} + \frac{i K_n}{\lambda_{nm}} \frac{\partial}{\partial r} \right) \psi_{nm}$$
$$+ \hat{e}_\theta \left(-\frac{\partial}{\partial r} - \frac{m K_n}{r \lambda_{nm}} \right) \psi_{nm} \tag{6}$$
$$+ \hat{e}_z \left(\frac{\lambda^2_{nm} - K^2_n}{\lambda_{nm}} \right) \psi_{nm},$$

$$\psi_{nm} = J_m(\gamma_{nm} r) \exp(im\theta + i K_n z)$$
$$\lambda_{nm} = \pm \left(\gamma^2_{nm} + K^2_n \right)^{1/2}, \quad K_n = \frac{2\pi n}{L}$$

$n = 0, \pm 1, \pm 2, \ldots\ldots.$

$m = 0, \pm 1, \pm 2, \ldots\ldots$

The functions $\vec{a}_{nm}$ satisfy $\vec{\nabla} \times \vec{a}_{nm} = \lambda_{nm} \vec{a}_{nm}$

γ_{nm} is determined from the boundary conditions Eq.(4) which becomes

$$R K_n \gamma_{nm} J'_m(\gamma_{nm} R) + m \lambda_{nm} J_m(\gamma_{nm} R) = 0 \tag{7}$$

The mechanical pressure p can be expressed as a function of $\vec{V}$ and $\vec{B}$ by taking the divergence of Eq.(1) and using Eq.(3) as

$$\nabla^2 p = -\nabla \cdot \left[(\vec{V} \cdot \vec{\nabla}) \vec{V} + (\vec{\nabla} \times \vec{B}) \times \vec{B} \right] \tag{8}$$

The dynamics can be described by taking the inner products of the Eqs.(1) and (2) with A^*_{nm} . We do this here by including only three modes (1,0), (0,1) and (1,1). The six complex, coupled nonlinear ordinary differential equations describing the temporal evolution of the triple-mode system are:

$$\frac{\partial \eta_a}{\partial t} = \frac{\lambda_b \lambda_c}{\lambda_a}(\lambda_c - \lambda_b)\, I\left[\eta_b \eta_c - \xi_b \xi_c\right] \tag{9}$$

$$\frac{\partial \eta_b}{\partial t} = \frac{\lambda_c \lambda_a}{\lambda_b}(\lambda_a - \lambda_c)\, I^*\left[\eta_c^* \eta_a - \xi_c^* \xi_a\right] \tag{10}$$

$$\frac{\partial \eta_c}{\partial t} = \frac{\lambda_a \lambda_b}{\lambda_c}(\lambda_b - \lambda_a)\, I^*\left[\eta_a \eta_b^* - \xi_a \xi_b^*\right] \tag{11}$$

$$\frac{\partial \xi_a}{\partial t} = \lambda_b \lambda_c\, I\left[\eta_b \xi_c - \eta_c \xi_b\right] \tag{12}$$

$$\frac{\partial \xi_b}{\partial t} = \lambda_c \lambda_a\, I^*\left[\eta_c^* \xi_a - \eta_a \xi_c^*\right] \tag{13}$$

$$\frac{\partial \xi_c}{\partial t} = \lambda_a \lambda_b\, I^*\left[\eta_a \xi_b^* - \eta_b^* \xi_a\right] \tag{14}$$

where $a \equiv (1,1)$, $b \equiv (1,0)$, $C \equiv (0,1)$

$$\lambda_a R = 3.11,\ \lambda_b R = 4.12,\ \lambda_c R = 3.83 \tag{15}$$

$$I = \int \vec{A}_a^* \cdot (\vec{A}_b \times \vec{A}_c)\, d^3 r$$

One has to use numerical techniques in order to solve Eqs.(9) to (14) in general. Before attempting that we discuss two simplified cases where some analytical progress can be made.

Case I

We disturb the system described by Eqs.(9)-(14) linearly from the equilibrium state ($\xi_{ao} = \eta_{ao}$, $\xi_{bo} = \eta_{bo}$ and $\xi_{co} = \eta_{co}$) such that

$$\begin{aligned} \eta &= \eta_o + \eta'(t)\,, \quad \eta' \ll \eta_o \\ \xi &= \xi_o + \xi'(t)\,, \quad \xi' \ll \xi_o \end{aligned} \tag{16}$$

for all modes. Let $\left.\begin{matrix} \eta'(t) \\ \xi'(t) \end{matrix}\right\} \sim e^{st}$

Therefore we are studying the time evolution of small departures from the equilibrium state. We find:

$$S = \pm i\,|I|\left[\lambda_a^2(\lambda_a-\lambda_b-\lambda_c)^2|\eta_{a0}|^2+\lambda_b^2(\lambda_b-\lambda_c-\lambda_a)^2|\eta_{b0}|^2 + \lambda_c^2(\lambda_c-\lambda_a-\lambda_b)^2|\eta_{c0}|^2\right]^{1/2} \tag{17}$$

Thus the system exhibits sinusoidal oscillations with a period which depends upon the equilibrium values of the fields. This result is also reproduced from the numerical scheme for solving Eq.(9) to Eq.(14), as shown in Fig.(1). In this Figure and Figure(4) we are using the notation

$$Y_1 = \mathrm{Re}\,\eta_a,\quad Y_2 = \mathrm{Im}\,\eta_a,\quad Y_3 = \mathrm{Re}\,\eta_b,\quad Y_4 = \mathrm{Im}\,\eta_b$$

$$Y_5 = \mathrm{Re}\,\eta_c,\quad Y_6 = \mathrm{Im}\,\eta_c,\quad Y_7 = \mathrm{Re}\,\xi_a,\quad Y_8 = \mathrm{Im}\,\xi_a$$

$$Y_9 = \mathrm{Re}\,\xi_b,\quad Y_{10} = \mathrm{Im}\,\xi_b,\quad Y_{11} = \mathrm{Re}\,\xi_c,\quad Y_{12} = \mathrm{Im}\,\xi_c$$

It would be instructive to estimate the time period $T = 2\pi/S$. Now ($\lambda\eta I$) has dimension of a velocity, and so let us write $\lambda_a^2\eta_a^2|I|^2 \equiv V_a^2$, the mean square velocity in the mode a. The time period T is given by:

$$T = 2\pi R\left[23.42\,V_a^2 + 7.95\,V_b^2 + 11.56\,V_c^2\right]^{-1/2} \tag{18}$$

For $V_a = V_{b,c} = V$, $T = \dfrac{0.95R}{V}$. Thus, for example, for $V \sim 10$ km/sec. and $R = 10^3$ km, one gets $T \sim 95$ secs. Quasiperiodic oscillations with a period of a minute or so have been observed in the microwave emission from coronal loops. It is possible that some of these oscillations result from such mode-mode interactions.

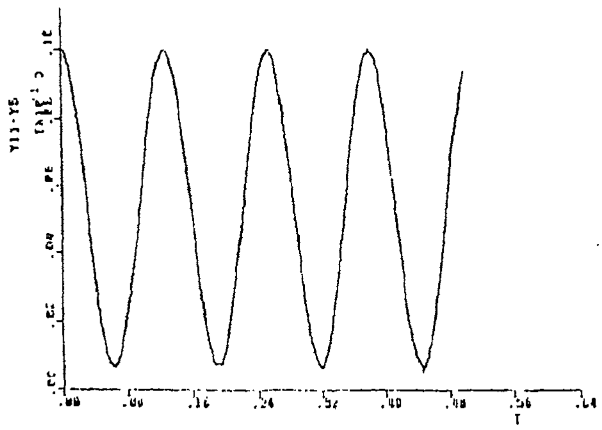

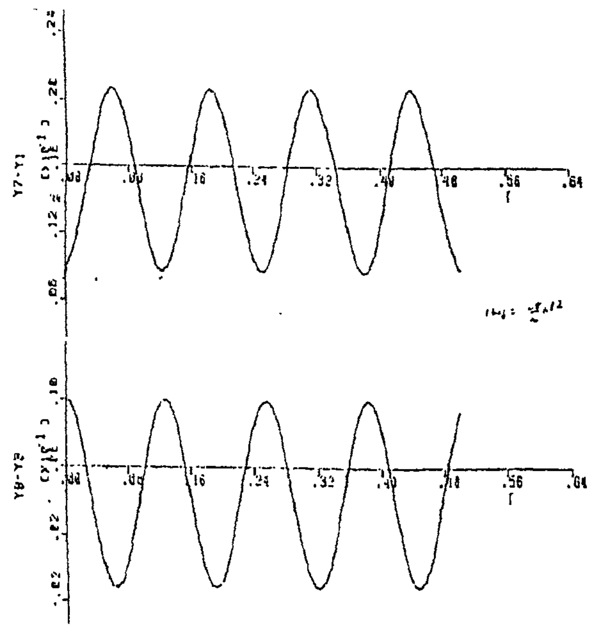

Fig. 1. The sinusoidal oscillations exhibited by a triple-mode system when disturbed linearly from its equilibrium state, showing (a) $Y_7 - Y_1$, (b) $Y_9 - Y_3$ and (c) $Y_{11} - Y_5$ as functions of time.

Case II The Pump Approximation

Another case of analytical tractability is when one of the three modes is more dominant than the other two. Here, it is assumed that the time evolution of the two weaker modes does not produce any significant change in the stronger mode, which is identified as the pump. Let us take $a \equiv (1,1)$ to be the dominant mode and therefore neglect all changes in (η_a, ξ_a). The system of six equations reduces to four with additional assumption $\eta_a = \xi_a$, to the following simplified form:

$$\frac{\partial \eta_b}{\partial t} = \frac{\lambda_c \lambda_a}{\lambda_b} (\lambda_a - \lambda_c) I^* [\eta_c^* - \xi_c^*] \eta_a \tag{19}$$

$$\frac{\partial \eta_c}{\partial t} = \frac{\lambda_a \lambda_b}{\lambda_c} (\lambda_b - \lambda_a) I^* [\eta_b^* - \xi_b^*] \eta_a \tag{20}$$

$$\frac{\partial \xi_b}{\partial t} = \lambda_c \lambda_a I^* [\eta_c^* - \xi_c^*] \eta_a \tag{21}$$

$$\frac{\partial \xi_c}{\partial t} = \lambda_a \lambda_b I^* [\xi_b^* - \eta_b^*] \eta_a \tag{22}$$

One can easily reduce these equations to find:

$$\frac{\partial^2 \eta_b}{\partial t^2} = P_1 \eta_b + P_2 \qquad (23)$$

$$\frac{\partial^2 \eta_c}{\partial t^2} = P_1' \eta_c + P_2'$$

$$\xi_b = \frac{\lambda_b}{\lambda_a - \lambda_c} (\eta_b - I_b), \; I_b = \eta_{bo} - \frac{(\lambda_a - \lambda_c)\xi_{bo}}{\lambda_b} \qquad (24)$$

$$\xi_c = \frac{\lambda_c}{\lambda_a - \lambda_b} (\eta_c - I_c), \; I_c = \eta_{co} + \frac{(\lambda_b - \lambda_a)\xi_{co}}{\lambda_c} \qquad (25)$$

$$P_1 = \lambda_a^2 (\lambda_a - \lambda_b - \lambda_c)^2 (I^*)^2 / |\eta_a|^2$$

$$P_2 = \lambda_a^2 \lambda_b (\lambda_a - \lambda_b - \lambda_c)(I^*)^2 / |\eta_a|^2 I_b \qquad (26)$$

$$P_1' = P_1$$

$$P_2' = \lambda_a^2 \lambda_c (\lambda_a - \lambda_b - \lambda_c)(I^*)^2 / |\eta_a|^2 I_c \qquad (27)$$

We observe from Eqs.(23) and (24) that all the four fields (η_b, ξ_b, η_c, ξ_c) exhibit sinusoidal oscillations with a frequency $\sqrt{-P_1}$ for specific initial values of (η_{bo}, ξ_{bo}) and (η_{co}, ξ_{co}) i.e. when $I_b = I_c = 0$ or when $\eta_{bo} = (\lambda_a - \lambda_c)\xi_{bo}/\lambda_b$ and $\eta_{co} = (\lambda_a - \lambda_b)\xi_{co}/\lambda_c$. The oscillation frequency found in the first case reduces to this under the approximation $\eta_a = \xi_a >> (\eta_b, \eta_c, \xi_b, \xi_c)$.

For $I_b \neq 0$ and $I_c \neq 0$, the solution of Eqs.(23) and (24) is given as

$$(t + t_o) = \frac{1}{\sqrt{P_2^2 - P_1 P_2}} \ln \left| \frac{\eta_b + \frac{P_2}{P_1} - \frac{1}{P_1}\sqrt{P_2^2 - P_1 P_2}}{\eta_b + \frac{P_2}{P_1} + \frac{1}{P_1}\sqrt{P_2^2 - P_1 P_2}} \right|$$

and

$$(t + t_o') = \frac{1}{\sqrt{P_2'^2 - P_1' P_2'}} \ln \left| \frac{\eta_c + \frac{P_2'}{P_1'} - \frac{1}{P_1'}\sqrt{P_2'^2 - P_1' P_2'}}{\eta_c + \frac{P_2'}{P_1'} + \frac{1}{P_1'}\sqrt{P_2'^2 - P_1' P_2'}} \right| \qquad (28)$$

where t_0 and t' are determined from the conditions $t = 0$, $\eta_b = \eta_{bo}$ and $\eta_c = \eta_{co}$.

A plot of (η_b, ξ_b, η_c, ξ_c) VS $T \equiv t|\eta_a|^2|I|^2$ is shown in Figure (2) for one set of initial conditions. The noticeable features of this plot are:

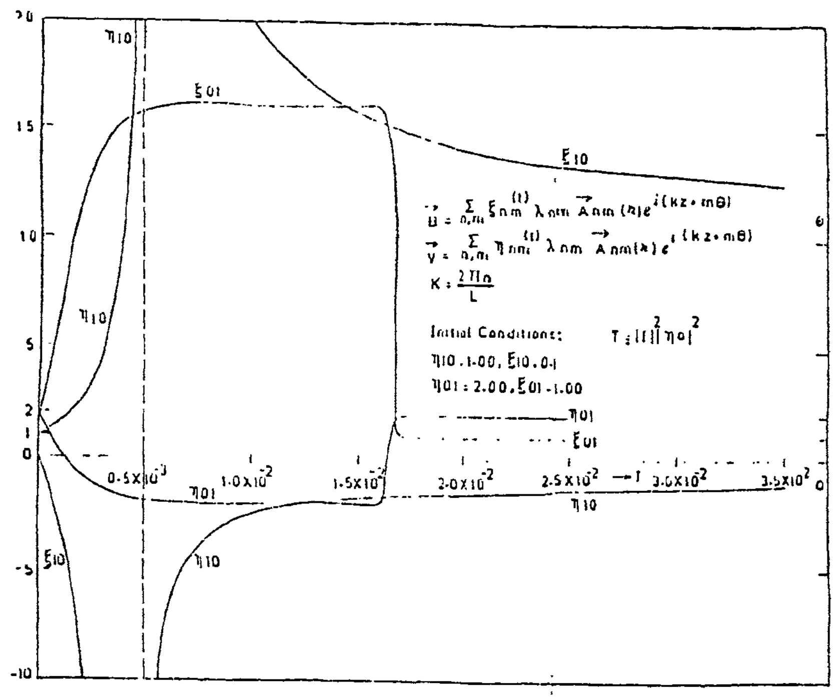

Fig. 2. The temporal evolution of the velocity and magnetic field coefficients (η_b, ξ_b) and (η_c, ξ_c) under the Pump approximation ($\eta_a >> \eta_b$, η_c and $\xi_a >> \xi_b$, ξ_c).

1. The velocity and magnetic field in the mode $b \equiv (1,0)$ go through zero at the same time.

2. The amplitudes η_b and ξ_b grow to a very large value before the reversal. These features are reminiscent of the observed simultaneous neutral lines of the velocity and magnetic field discussed by Athay & Klimchuk (1987).

3. Asymptotically the magnetic field ξ_b settles to a value much larger than its initial value. The velocity amplitude η_b settles to a value which is negative of its initial value.

4. The fields in the mode $c \equiv (0,1)$ undergo growth, plateau and decay.
5. Asymptotically, the fields ξ_c and η_c attain back their initial values.
6. The large time gradients of the fields may help expalin micro-and nanoflares since they correspond to impulsive small scale release of energy.

Another quantity of interest in an ideal MHD system is the correlation coefficient γ defined as:

$$\gamma = \left[\frac{1}{2}\int \vec{V}\cdot\vec{B}\, d^3r\right] \Big/ \left[\frac{1}{2}\int (V^2 + B^2)\, d^3r\right] \tag{29}$$

where time variations (Fig.3) are a measure of the error involved in truncating the full system, for which γ would be constant.

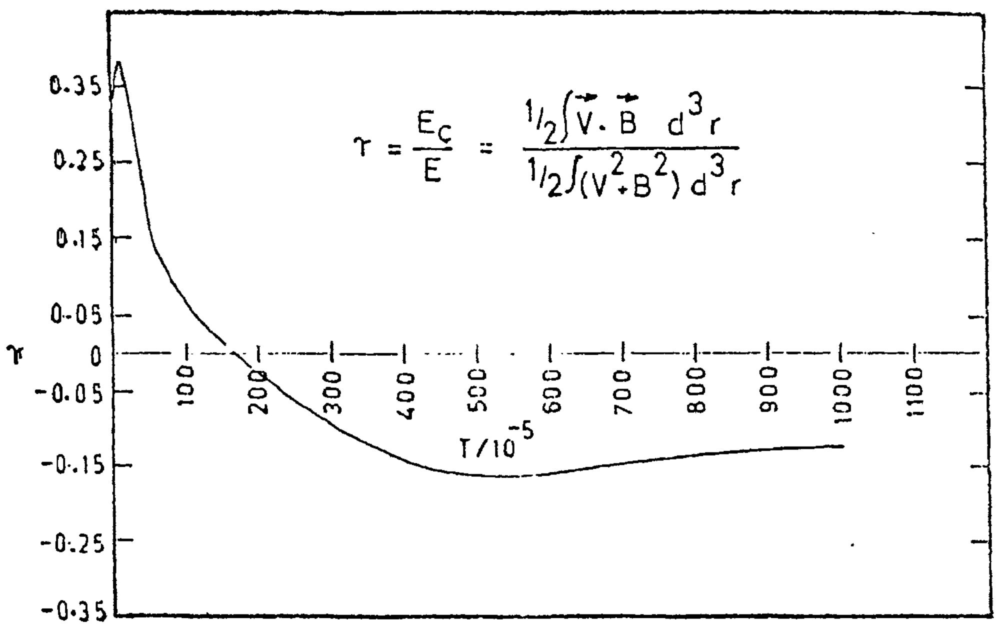

Fig.3. Variation of the correlation coefficient γ with time.

The spatial variation of the fields is given by Eq.(6). It is interesting to note that the three-mode representation discussed here, reduces to only one mode $b \equiv (1,0)$ when averaged over the angular coordinate θ . This $b \equiv (1,0)$ mode is the one that shows simultaneous reversal in the velocity and magnetic field and may therefore be related to the observed fields.

We have made some preliminary attempts to solve the exact set of Eqs.(9)-(14) for general initial conditions. One expects the fields to vary in a highly nonlinear manner. An example of the temporal variation of the fields is presented in Fig.(4).

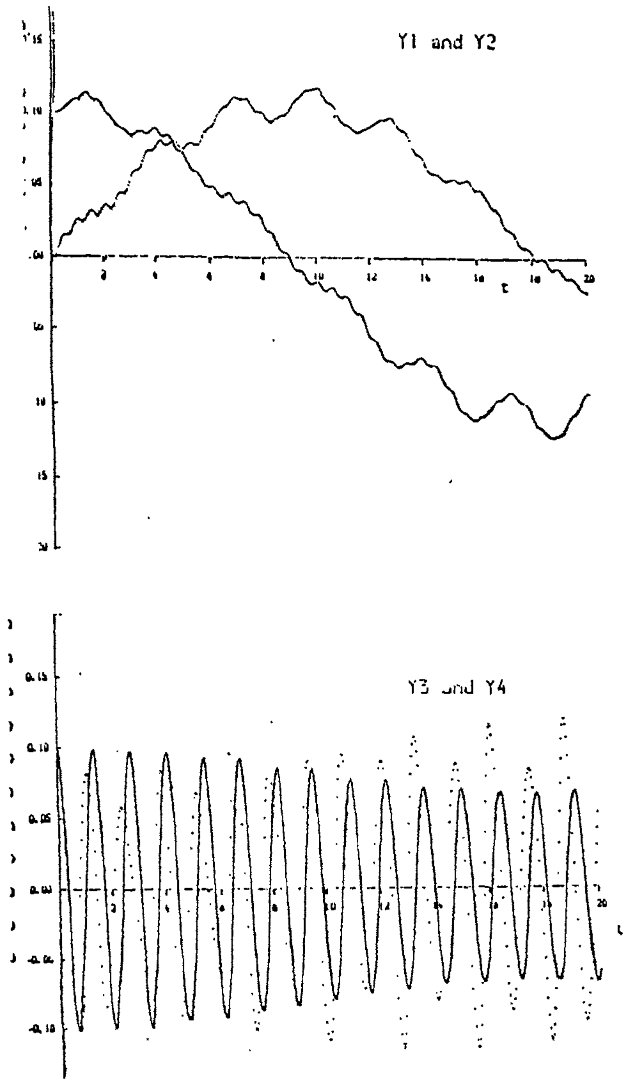

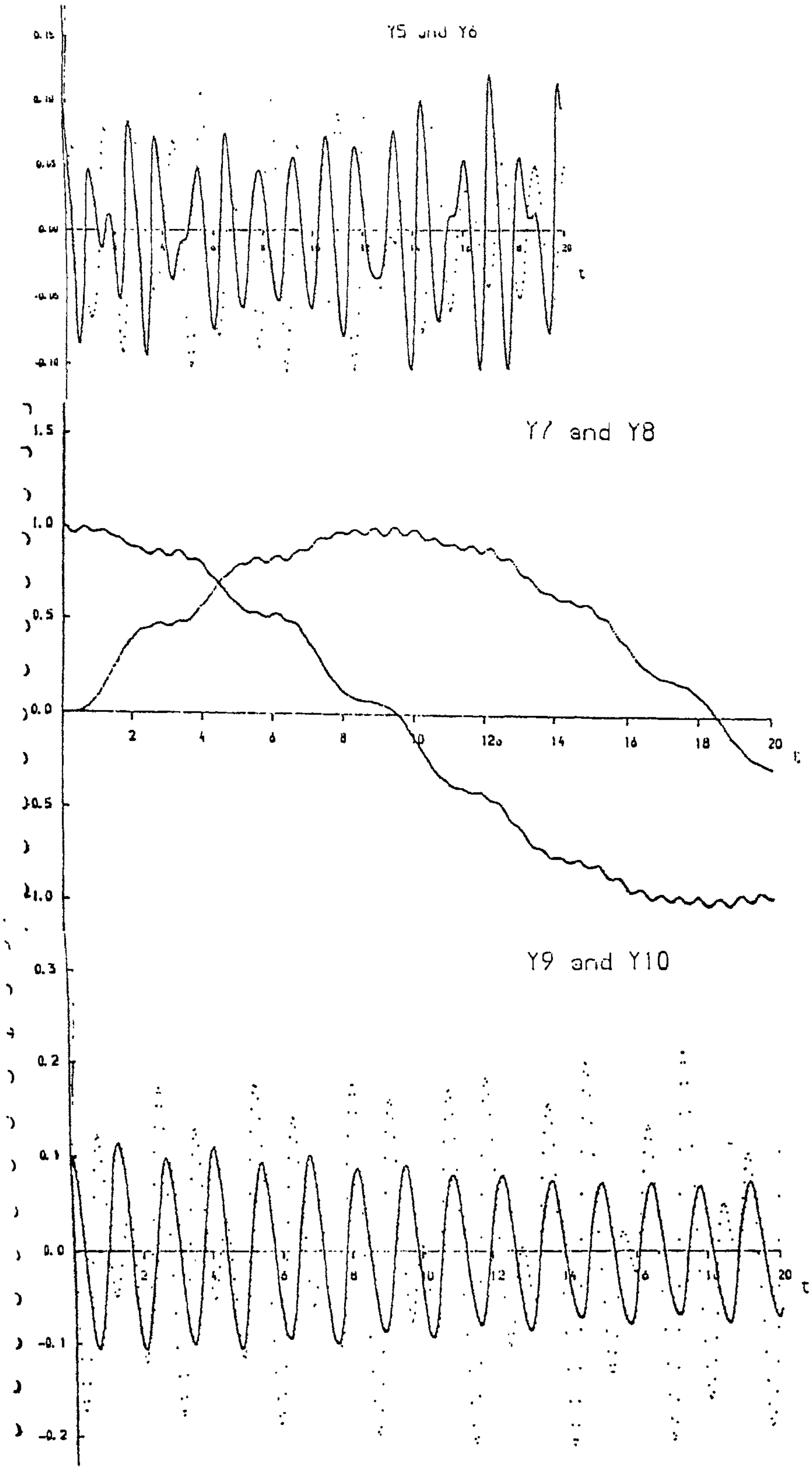

Fig. 4. Temporal evolution of the velocity and magnetic field coefficients in triple mode interaction system for arbitrary initial conditions.

It is quite clear that there is no simple way of interpreting this bebahviour, which is caused by superposition of the separate modes of oscillation. When more modes are added, it is possible that the system may show chaotic behaviour. The total energy, the magnetic helicity and the total cross helicity are found to remain constant with time as one expects for an ideal MHD system.

Acknowledgement

One of the authors (V.K.) is grateful to Dr.Alan Hood for many very useful discussions during the course of this work.

References

Athay,R.G. and Klimchuk,J.A., 1987 Ap.J. **318**, 437.
Krishan,V. 1983 Sol. Phys. **88**, 155.
Krishan,V. 1985 Sol. Phys. **95**, 269.
Pouquet,A. et al 1984, in 'Turbulence and chaotic phenomena in fluids' Ed.T.Tatsumi pp.501.
Priest,E.R. 1982 Solar Magneto-hydrodynamics D.Reidel.